High Power Laser Science and Engineering, (2021), Vol. 9, e57, 15 pages.
doi: 10.1017/hpl.2021.39

HIGH POWER LASER SCIENCE AND ENGINEERING

REVIEW

Free electron lasers driven by plasma accelerators: status and near-term prospects

C. Emma[1], J. Van Tilborg[2], R. Assmann[3], S. Barber[2], A. Cianchi[4], S. Corde[5], M. E. Couprie[6], R. D'Arcy[3], M. Ferrario[4], A. F. Habib[7], B. Hidding[7], M. J. Hogan[1], C. B. Schroeder[2], A. Marinelli[1], M. Labat[6], R. Li[8], J. Liu[8], A. Loulergue[6], J. Osterhoff[3], A. R. Maier[3], B. W. J. McNeil[9,10], and W. Wang[8]

[1] *SLAC National Accelerator Laboratory, Menlo Park, CA 94025, USA*

[2] *BELLA Center, Lawrence Berkeley National Laboratory, Berkeley, CA 94720, USA*

[3] *Deutsches Elektronen-Synchrotron DESY, 22607 Hamburg, Germany*

[4] *INFN-LNF, 00044 Frascati, Italy*

[5] *LOA, ENSTA Paris, CNRS, Ecole Polytechnique, Institut Polytechnique de Paris, 91762 Palaiseau, France*

[6] *Synchrotron SOLEIL, L'Orme des Merisiers, Saint-Aubin, 91192 Gif-sur-Yvette, France*

[7] *Scottish Centre for the Application of Plasma-Based Accelerators SCAPA, Department of Physics, University of Strathclyde, Scottish Universities Physics Alliance SUPA, Glasgow G1 1XQ, UK*

[8] *Shanghai Institute of Optics and Fine Mechanics, Chinese Academy of Sciences, Shanghai 201800, China*

[9] *Department of Physics, University of Strathclyde, Scottish Universities Physics Alliance SUPA, Glasgow G1 1XQ, UK*

[10] *Cockcroft Institute, Warrington WA4 4AD, UK*

(Received 15 July 2021; revised 24 August 2021; accepted 27 August 2021)

Abstract

Owing to their ultra-high accelerating gradients, combined with injection inside micrometer-scale accelerating wakefield buckets, plasma-based accelerators hold great potential to drive a new generation of free-electron lasers (FELs). Indeed, the first demonstration of plasma-driven FEL gain was reported recently, representing a major milestone for the field. Several groups around the world are pursuing these novel light sources, with methodology varying in the use of wakefield driver (laser-driven or beam-driven), plasma structure, phase-space manipulation, beamline design, and undulator technology, among others. This paper presents our best attempt to provide a comprehensive overview of the global community efforts towards plasma-based FEL research and development.

Keywords: plasma accelerators; free electron lasers; novel light sources

1. Introduction

In plasma-based accelerators, the ionized plasma in a gas cell or gas jet can sustain ultra-high accelerating fields of the order of 10–100 GV/m, which is 2–3 orders of magnitude larger than in conventional radiofrequency (RF)-based accelerators. It is this high field that enables acceleration by multi-gigaelectronvolt energies in centimeter-scale plasmas. At densities of order $10^{15}-10^{18}$ cm^{-3}, the plasma wakefield can be best described as having a longitudinally oscillating density profile at the plasma wavelength λ_p, trailing a driver that propagates close to the vacuum speed of light. Here $\lambda\,[\mu\mathrm{m}] = 33/\sqrt{n\left[10^{18}\,\mathrm{cm}^{-3}\right]}$, which reveals the scale length of the wakefield period to be of the order of 100 μm. The rapid acceleration of background-injected electrons to relativistic energies, inside the micrometer-sized structured plasma environment, allows the trapped electron beam to remain short, dense, and free of significant space-charge-driven emittance degradation. These high-brightness beams position plasma-based accelerators well as enabler of the advanced-accelerator free-electron laser (FEL)[1].

The driver of the plasma wakefield can either be (i) an ultra-intense laser pulse[2,3], at tens of femtoseconds duration

Correspondence to: C. Emma, SLAC National Accelerator Laboratory, Menlo Park, CA 94025, USA; J. Van Tilborg, BELLA Center, Lawrence Berkeley National Laboratory, Berkeley, CA 94720, USA. Email: cemma@slac.stanford.edu (C. Emma); jvantilborg@lbl.gov (J. Van Tilborg)

and focused to approximately 20 μm spot sizes to reach 10^{18} W/cm^2 laser intensities, or (ii) a dense relativistic electron beam, also of sub-picosecond duration and kiloamp-level peak current[4–6]. Differences exist between these so-called laser-driven and beam-driven wakefield accelerator concepts, such as facility requirements, intrinsic driver–wakefield dephasing limitation, and driver guiding conditions, but the core concepts of wakefield structure, background electron injection physics, and the subsequent production of high-quality electron beams share many similarities between the two approaches.

The quality of the electron beams can be assessed based on the six-dimensional phase space, including final energy, energy spread, charge, bunch length, beam divergence, transverse source size, repetition rate, as well as long-term and shot-to-shot stability. For laser-driven wakefield accelerators (LWFAs), energies up to 8 GeV energy gain have been reported[7], as well as per-mille level energy spread[8], 10–100 pC charge, few-femtosecond beam duration[9], sub-millirad divergence, few-micrometer source size[10], and repetition rates up to 10 Hz (and planned for kilohertz). For beam-driven wakefield accelerators (PWFAs), energies up to 84 GeV (42 GeV energy gain) have been reported[11], as well as per-mille-level energy spread[12,13], 10–100 pC charge, tens of femtosecond beam duration[14,15], micrometer-level normalized emittance[16], 10 μm level source size, and few hertz repetition rates. With these properties already having been demonstrated, there are a growing number of experimental programs interested in using these electron beams to drive next-generation light sources. In this paper, we discuss the status and prospects of the existing facilities and university groups that are actively pursuing plasma-accelerator-driven light source development on the path towards an X-ray free-electron laser (X-FEL).

The quality of the plasma-accelerated electron beams driving the FEL process is essential for determining the properties of the emitted FEL radiation. Many of these properties are described by the 1D model of the FEL interaction and are related to the Pierce parameter ρ[17]:

$$\rho = \left(\frac{1}{16} \frac{Q/\tau}{I_A} \frac{K_0^2 [JJ]^2}{\gamma^3 \sigma_r^2 k_u^2} \right)^{1/3}, \quad (1)$$

with Q the beam charge, τ the beam duration (such that $I = Q/\tau$ represents the beam current), $I_A \approx 17$ kA the Alfvén current, $[JJ]$ a K-dependent parameter of order unity, σ_r the transverse electron beam size, and $\lambda_u = 2\pi/k_u$ the undulator period. The Pierce parameter determines the one-dimensional (1D) gain length, which in turn can be applied for three-dimensional (3D) scaling, and gives an estimate of the saturation power through[18]

$$L_{G,1D} = \frac{\lambda_u}{4\sqrt{3}\pi\rho} \rightarrow L_{G,3D} = L_{G,1D}(1+\Lambda), \quad (2)$$

$$P_{sat} \approx 1.6\rho \left(\frac{L_{G,1D}}{L_{G,3D}} \right)^2 P_{beam}. \quad (3)$$

Here the beam power is given by P_{beam} [TW] $= E$[GeV]I[kA], and Λ represents several factors that could hinder FEL lasing and increase the gain length, such as energy spread, diffraction, and emittance. Fitting formulas available in the literature[18] allow one to calculate $L_{G,3D}$. For example, a 500 MeV electron beam at 1% energy spread, 50 pC charge in 5 fs duration, focused to a beamsize of 20 μm inside a $K = 1.26$ undulator at $\lambda_u = 1.8$ cm, will yield a 8.3 cm 1D gain length and a 48 cm corrected 3D gain length, at photon energy 74 eV. Note that such e-beam parameters are within reach of demonstrated plasma-based facilities, and highlight the potential of these centimeter-scale accelerators for dramatically reducing the size and cost of advanced light sources such as FELs. As discussed in the core sections of the text, several mitigation strategies can be applied to trade-off phase-space parameters and bring the 3D gain length down further, and photon energy higher towards hard X-ray operation.

In this paper, we highlight the efforts of eight state-of-the-art plasma-accelerator facilities and groups, four utilizing the LWFA and four utilizing the PWFA approach to realize a plasma-driven FEL. We include an introduction to the specific methodology being pursued by each experiment, an experimental design, the current status of the efforts, and each facility and group's future vision for progress. As illustrated by Tables 1 and 2 the parameter space spanned by the respective facilities and groups covers a broad range of electron beam energies and a spectrum of FEL wavelengths spanning from UV to hard X-rays. Each experimental program is aimed at addressing a number of the key challenges facing plasma FEL operation: demonstration of plasma-FEL gain, achieving stable operation in a plasma FEL, reaching high average power in a plasma FEL, demonstrating hard X-ray operation, adding capabilities to existing FEL by generating attosecond pulses and finally creating an operational user facility dedicated to science with plasma-driven FELs. These key challenges are being tackled by utilizing different undulator technology and different FEL operating modes leveraging the inherent properties of plasma-accelerated electron beams including high peak current, short bunch length, strong time-energy chirps, and potentially ultra-low emittance and ultra-high brightness. Following the discussion of individual facility and group efforts we conclude by providing an outlook for the development of plasma-driven FELs as a near-term application of plasma accelerators.

2. SLAC, FACET-II

The FACET-II facility for advanced accelerator experimental tests at the SLAC National Accelerator Laboratory[19],

https://doi.org/10.1017/hpl.2021.39 Published online by Cambridge University Press

Table 1. Summary of parameters for the facilities discussed in the text utilizing a laser-driven approach to plasma-FEL operation.

	COXINEL	DESY-LUX	SIOM	LBNL-BELLA
Charge density [pC/MeV]	0.5	4	1–5	2
Repetition rate [Hz]	1–10	1	1–5	5
Mean energy [GeV]	0.18–0.4	0.3	0.84	0.1–0.3
Slice energy spread RMS [%]	NA	0.5	0.24–0.4	0.2–1
Charge [pC]	NA	50	8–25	25
Emittance [mm·mrad]	1	1.5 (horz.), 0.3 (vert.)	0.4	0.3–1
FEL wavelength [nm]	UV-VUV	100	6–10	80
Undulator technology	Cryo-PMU	Cryo-PMU	Planar and TGU	Planar + strong focusing
FEL operation modes	Decompression + seeding	Decompression + SASE	SASE, transverse decompression	Decompression + seeding
Key challenge pursued	Demonstrate FEL gain	Demonstrate FEL gain	Demonstrate FEL gain	Demonstrate FEL gain

FEL, free-electron laser; PMU, permanent magnet undulator; RMS, root mean square; SASE, self-amplification of spontaneous radiation; TGU, transverse gradient undulator.

Table 2. Summary of parameters for the facilities discussed in the text utilizing a beam-driven approach to plasma-FEL operation. We note that both Strathclyde and EuPRAXIA are also aiming to study multiple plasma-based FEL approaches including hybrid LWFA–PWFA configurations. Facilities/groups labeled with an asterisk have not yet begun experimental operation and for those the target parameters have been listed.

	SLAC FACET-II*	DESY - FLASHForward	Strathclyde*	EuPRAXIA at SPARC LAB*
Peak current [kA]	10–500	1	1–100	4
Repetition rate [Hz]	1	10 (10^4 after future upgrades)	Variable	10
Mean energy [GeV]	5–10	1	1–5	1–5
Slice energy spread RMS [%]	0.1–1	0.15	0.01–2	0.75
Charge [pC]	10–100	100	0.1–500	30
Emittance [mm·mrad]	1–10	1–20	0.01–1	1
FEL wavelength [nm]	10–50	Soft X-rays	Hard X-rays	4
FEL operation modes	Compression + pre-bunching	SASE	Multiple	SASE
Key challenge pursued	Attosecond FEL pulses	High average power FEL	Hard X-ray FEL gain	Plasma-FEL user facility

FEL, free-electron laser; RMS, root mean square; SASE, self-amplification of spontaneous radiation.

delivers 10 GeV, multi-kiloamp current electron bunches for a suite of advanced accelerator and coherent radiation experiments. A detailed description of the FACET facility including e-beam parameters can be found in Ref. [19], and a discussion of the plasma wakefield science program is given in Ref. [20]. The facility will operate with either a single drive bunch or a two-bunch drive-witness configuration. Both configurations generate the electron beams in a photocathode RF gun and compress them to few-micrometer bunch length with nanocoulomb-level charge before delivering them to the experimental area which is shown schematically in Figure 1. Two separate plasma sources, one meter scale with densities $O(10^{16}\ \mathrm{cm}^{-3})$ based on laser or field ionization of Li-vapor[21,22], and one centimeter scale with densities $O(10^{18}\ \mathrm{cm}^{-3})$ based on gas jet ionization will be available for separately serving experiments. The PWFA experiments will include testing different ultra-low emittance plasma injection schemes relevant for FEL applications[23,24].

The concept behind the FACET-II X-FEL experiment, termed Plasma-driven Attosecond X-ray source (PAX), was first outlined in Ref. [25]. The experiment will leverage the strong chirps naturally present in plasma-accelerated beams to further compress the witness bunch in a weak compressor after the exit of the plasma stage to a single high current spike of attosecond duration. This attosecond current spike has a substantial (percent-level) bunching factor at soft X-ray wavelengths and can generate high-power attosecond pulses of coherent X-rays in a downstream bend or undulator magnet. This approach to plasma-driven X-FEL emission is motivated by the order-of-magnitude increased tolerances of this method to emittance, energy spread, and pointing jitter compared with a regular self-amplification of spontaneous radiation (SASE) X-FEL starting from noise. Furthermore, this approach opens the possibility of using plasma based FELs to generate tens of attosecond long X-ray pulses with terawatt peak power, an order of magnitude shorter than what is possible with existing attosecond SASE X-FELs[26,27]. Achieving this goal would not only substantially decrease the physical footprint of an X-FEL facility, a major motivator for pursuing plasma-based FEL technology, but also add a new capability to the X-FEL light source attracting interest from the X-FEL scientific user community.

The experimental effort aimed at demonstrating this concept is planned in two stages. The first stage will target coherent XUV generation using a two-bunch setup, with both bunches generated by the RF photoinjector and injected into the Li vapor plasma source. A high-charge $Q = 1.5$ nC drive beam drives a nonlinear blowout in which the low charge $Q \sim 10$ pC witness bunch is strongly chirped and subsequently compressed in a downstream chicane with $R_{56} \sim 100\ \mu$m to a final bunch length ~ 40 nm full width at

https://doi.org/10.1017/hpl.2021.39 Published online by Cambridge University Press

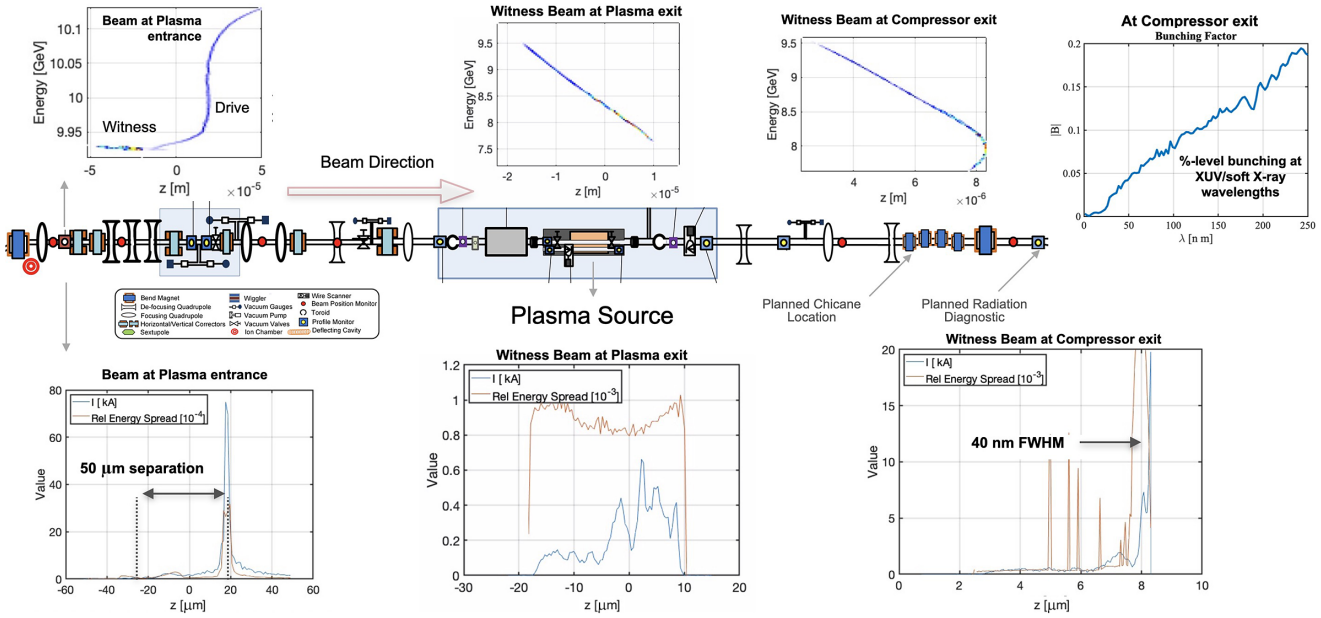

Figure 1. Schematic of the FACET-II experimental area with the planned location of an additional small chicane and radiation diagnostic to be used for X-FEL experiments. The simulated longitudinal phase space evolution shows the compression of the electron beam to attosecond duration with percent-level bunching at XUV/soft X-ray wavelengths.

half maximum (FWHM); see Figure 1. Coherent synchrotron radiation will be extracted from the last bend magnet in the chicane (at the planned chicane location in Figure 1) and the spectrum will be analyzed using an XUV spectrometer (at the planned radiation diagnostic location) to demonstrate attosecond compression of a plasma accelerated e-beam. The second stage will use a single drive bunch of $Q = 2$ nC incident on the high-density gas jet plasma source to generate a higher charge $Q \sim 100$ pC witness beam using a plasma injection scheme such as density downramp injection[8,28–30]. The ultrahigh brightness witness beam will be compressed to shorter final bunch length $\sigma_z \sim 10$ nm thereby extending the photon energy range for coherent emission from XUV to soft X-rays. In the final stage of the experiment, we anticipate installing a short few-period undulator, to increase the peak power of the emitted X-ray pulses and characterize the properties and pulse duration of the emitted attosecond X-rays. This experimental proposal was approved by the FACET-II program advisory committee in October 2020 and the experimental planning is currently underway to accommodate the installation of the chicane and XUV spectrometer in the FACET-II beamline. With the FACET-II facility currently initiating its user-assisted commissioning phase, initial beam studies related to this experiment are planned to start in the fall of 2021.

3. COXINEL

The COXINEL (COherent Xray source INferred from Electrons accelerated by Laser) in France aims at qualifying present laser plasma acceleration experiments with an FEL application. As the divergence, the energy spread and the charge densities do not reach values as currently achieved on conventional linear accelerators (LINACs), the COXINEL key concept relies on an innovative electron beam longitudinal and transverse manipulation in the transport towards an undulator. The COXINEL line has been designed and built at Synchrotron SOLEIL[31–33], for exploiting the electron beam generated and accelerated using the Ti:sapphire laser system 'Salle Jaune' at Laboratoire d'Optique Appliquée (LOA), delivering 1.5 J, 30 fs FWHM pulses on target. The divergence is mitigated close to the source via strong focusing provided by a triplet of high-gradient permanent magnet quadrupoles of variable strength (so-called QUAPEVA)[34–36]. A magnetic chicane then longitudinally stretches the beam, sorts electrons in energy, and selects the energy range of interest via a removable and adjustable slit mounted in the middle of the chicane[37]. A second set of quadrupoles chromatically matches the beam inside an undulator, taking advantage of the correlation between energy and longitudinal position introduced in the chicane[38–40]. Undulator radiation is generated in the UV and VUV bands thanks to cryogenic permanent magnet undulators (the 2 m long CPMU18 operated at room temperature and the 3 m long CPMU15)[41–43]. The beamline is fully equipped with diagnostics such as current transformers, cavity beam position monitors, and imaging scintillator screens[44]. The laser-plasma accelerator (LPA) operated in the robust ionization injection regime[45,46] with a supersonic jet of He-N_2 gas mixture, providing electrons with energies up to 250 MeV, 0.5 pC/MeV charge density,

https://doi.org/10.1017/hpl.2021.39 Published online by Cambridge University Press

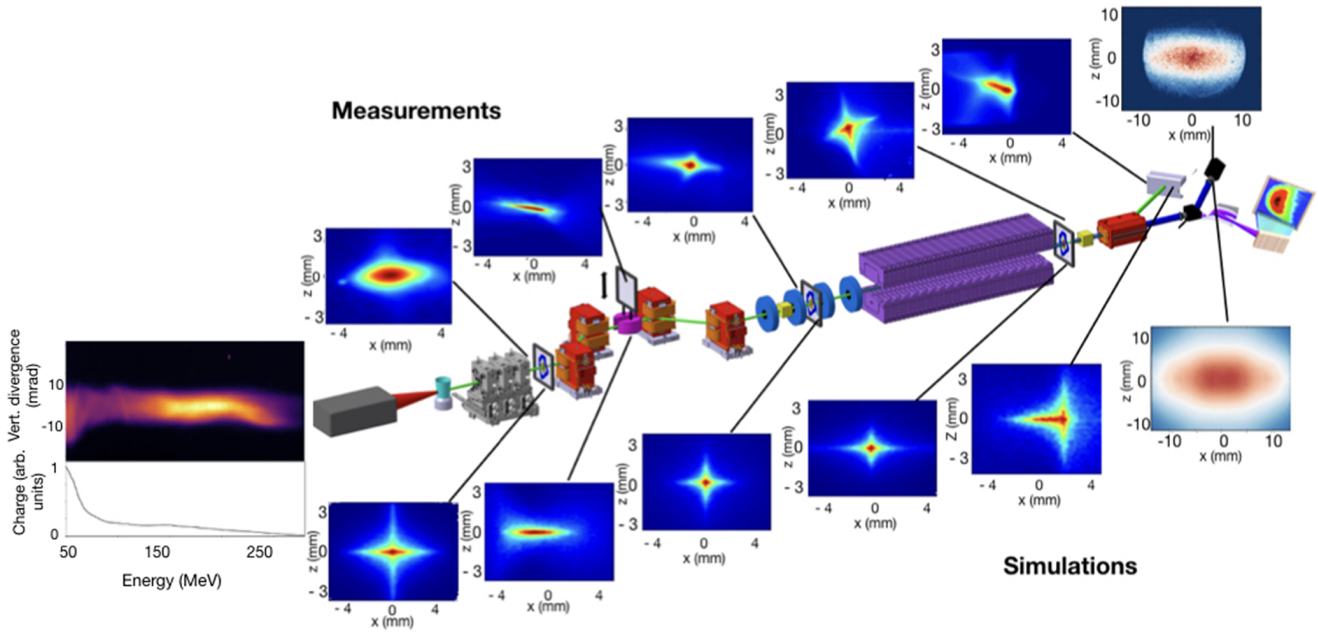

Figure 2. COXINEL electron and photon beam measurements compared to simulations. Left: Electron beam spectrometer measurements and transverse distributions along the screens (top: measurements; bottom: simulations using the measured electron beam distribution as an input). Right: Undulator radiation transverse pattern (measured with a CCD camera and modeled using the transported electron beam without electron energy selection).

and few millirad divergence (1.2–2 mrad root mean square (RMS)). The electron beam is properly transported along the line[40,47,48], mitigating alignment residual errors and electron beam pointing drifts thanks to the beam position alignment compensation (see Figure 2). The undulator radiation has been characterized with the CCD camera and a UV spectrometer. It exhibits the typical moon shape pattern (quadratic dependence of the resonant wavelength versus the observation angle), characteristic of undulator radiation[49], and its linewidth can be controlled thanks to the energy selection in the chicane.

The COXINEL line has been designed with baseline reference parameters (1 π·mm·mrad total normalized RMS emittance, 1 mrad RMS divergence, 1% RMS relative energy spread with a 1 μm RMS bunch length, 34 pC charge, and 4 kA peak current for 180–400 MeV). In the seeded configuration, it can lead to spectral interference between the coherently emitted radiation and the input seed, allowing for a full temporal reconstruction of the FEL pulse amplitude and phase distributions[50]. Presently, the main limitation for the FEL demonstration comes from the achieved electron beam parameters, as confirmed by sensitivity studies[51]. Improved electron beam performance is foreseen with the LAPLACE project (LAser PLAsma acceleration CEnter), led by LOA.

4. DESY, FLASHForward

The FLASHForward experimental facility[52] is a high-performance test-bed for precision plasma-wakefield research housed at the FLASH FEL complex[53], aiming to accelerate high-quality electron beams to gigaelectronvolts-levels in a few centimeters of ionized gas. The electrons to be accelerated will either be injected internally from the plasma background via density-downramp injection or externally from the FLASH superconducting RF front end. In both cases the wakefield is driven by nanocolulomb-level electron beams produced by the photocathode gun, accelerated in the superconducting RF LINAC modules to gigaelectronvolt energies, and compressed to O(100 fs RMS) lengths and multi-kiloamp peak currents in a series of chicanes and doglegs. The electron beams propagate through a windowless beamline, facilitated by a series of differential pumping systems, and then interact with a plasma contained within a gas cell, generated either by a high-voltage discharge or a high-intensity 25 TW Ti:sapphire laser pulse.

The first marquee goal of FLASHForward is to demonstrate high-fidelity acceleration of electron bunches in gigavolt per meter gradient wakes with final beam quality sufficient to produce gain in an FEL, synergistic with the parallel drive at DESY of generating FEL gain with a laser-driven plasma-accelerator source[54]. This is made possible at FLASHForward in large part due to the exquisite stability of the FEL-standard FLASH front end. Great progress has been made in this direction in recent years via multiple branches: developing techniques to improve beam quality after plasma acceleration[55], diagnostics to better understand the plasma-wakefield process in order to optimize it[56], and finally demonstrator experiments utilizing these techniques

https://doi.org/10.1017/hpl.2021.39 Published online by Cambridge University Press

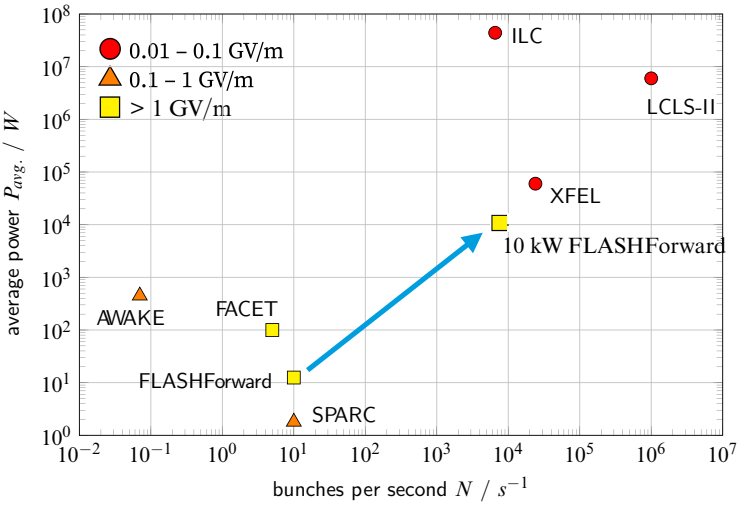

Figure 3. Average power as a function of the number of drive bunches per second at a range of existing or planned plasma-wakefield research facilities (bottom left corner) and photon-science and high-energy-physics user facilities (top right). The blue arrow represents the leap towards a beam-driven plasma-based FEL by using high-average-power upgrades to FLASHForward as a gateway.

for the preservation of beam quality[12]. This combined pillar of research will continue until a single highly efficient stage capable of simultaneous preservation of transverse (normalized emittance) and longitudinal (energy spread) quality over large energy gain is demonstrated.

The subsequent goal of FLASHForward is to take the idealized single plasma stage and operate it with the repetition rates and average powers required to push plasma-accelerator research in the direction needed to match and even exceed the brilliances of current FEL facilities. The FLASH LINAC operates at a 10 Hz macro-pulse rate, with typical FLASHForward operating conditions utilizing a single bunch per 800 μs RF flat-top. The FLASH gun and LINAC, however, can operate in a burst mode at up to 3 MHz micro-pulse repetition rates. At full capacity, the FLASH bunch-train structure corresponds to 10 kW of average power, orders of magnitude higher than drivers available to other state-of-the-art and planned laser-driven and beam-driven plasma-accelerator experiments (see Figure 1).

Based on the DESY plasma-accelerator roadmap, the route towards utilizing the full 10 kW of average power would be split into three phases: (1) answer the essential physics questions, such as how quickly the wakefield process can be repeated and what technology we need to develop to repeat the process at that rate; (2) demonstrate sustained operation (10–20 bunches) at a repetition rate conducive with the majority of demands of current FEL users, e.g., 10–100 kHz; (3) access the full megahertz-burst-mode functionality of FLASH to demonstrate kilowatt-level plasma acceleration (Figure 1). The advantage of this staggered approach is that significant progress may be made in the early stages whilst operating at relatively low average power, i.e., at high repetition rates in short bursts. Once higher average powers in plasma can be technically managed, however, a 10 kW FLASHForward would represent a high-average-power energy-boosting upgrade to the FLASH FEL facility, enabling access to, e.g., the oxygen K-edge at 2.33 nm, a credible and broad-impact advertisement for the field as well as its application to future projects.

5. DESY, LUX

The LUX facility[57], jointly operated by DESY and the University of Hamburg, follows the mission of developing laser-plasma acceleration towards a drive technology ready for applications by combining the state-of-the-art in modern accelerator technology and diagnostics with the novel concepts of plasma-based accelerators. A plasma-driven FEL is arguably the most prominent application for this novel technology. Demonstrating FEL gain is therefore an important goal and serves as a challenging benchmark for the facility's capability to control the plasma accelerator and provide FEL-quality electron beams.

Since the commissioning in 2016[57], the LUX beamline has been upgraded continuously. It is operated by the Angus 100 TW-class Ti:sapphire drive laser at 1 Hz repetition rate. The plasma target is based on a hydrogen-filled continuous-flow capillary to provide reproducible conditions for every laser shot. The whole beamline is build following the same vacuum standards as the user facilities operated on campus. Tightly integrated into an accelerator-grade control system, a rich set of data, combining electron and laser data as well as machine status and lab conditions, is recorded for every single shot, monitored live and stored for post-analysis.

With the demonstration of continuous 24-hour operation of the LUX plasma accelerator[54] a major milestone was achieved in 2020. Based on previous work, which studied the thermal management and spatiotemporal couplings of the

https://doi.org/10.1017/hpl.2021.39 Published online by Cambridge University Press

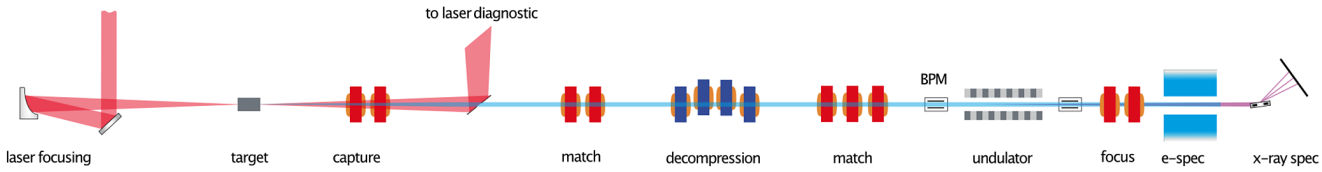

Figure 4. Schematic view of the LUX beamline after upgrade. For simplicity, diagnostics, such as electron beam profile monitors, are not shown.

drive laser pulse from heat-induced deformations of the laser compressor gratings[58,59], more than 100,000 consecutive laser-plasma electron beams could be demonstrated. The capability to continuously deliver drive laser pulses, enables the correlation of drive laser and electron beam parameters to identify optimized working points and, thus, formed the basis for a series of following studies that improved the plasma target design and electron beam quality.

A new target, which is based on localized ionization injection and optimizes beam loading throughout the whole acceleration process, now provides 1%-level energy spread at approximately 4 pC/MeV spectral density[60]. Those high-quality beams are, however, not delivered with every shot. A detailed analysis of electron and laser data provided insight into the main mechanisms leading to deviations from the optimum settings and could identify the main laser properties responsible for shot-to-shot variations in the electron beams. This analysis provides a clear path for further improvements to the laser system and to more reliably provide high-quality electron beams.

With increasing complexity of the target and the acceleration dynamics it becomes ever more difficult to identify an optimum working point for the plasma accelerator and then to reach this working point reliably on a day-to-day basis. To address this problem, machine learning techniques such as Bayesian optimization have been applied to the LUX accelerator[61] to, first, identify an optimum accelerator setting using particle-in-cell (PIC) simulations. A key factor for this study was the recent advances in the PIC domain, that enabled an accurate modeling of the experiment conditions in combination with a fast execution time and numerical accuracy[62,63]. The same algorithms then could be used in the experiment to autonomously tune the accelerator to the predicted high quality 1%-level energy spread beams.

The quality of the generated beams will benefit a future proof-of-principle experiment to demonstrate gain from a plasma electron beam. The LUX beamline is currently being upgraded (Figure 4) to perform such an experiment. The experiment will closely follow the so-called decompression scheme proposed in Refs. [64–66] operating in the SASE regime starting from noise. For the FEL amplification to set in, it is crucial for the electron beam energy spread σ_γ/γ to be smaller than the Pierce parameter ρ. The Pierce parameter combines electron beam and undulator properties into a normalized scaling quantity and is typically on the order of $<1\%$. The decompression scheme is based on a two-fold approach: first, reduce the energy spread of the electron beam, and, second, increase the Pierce parameter by optimizing the experiment design. Plasma-generated electron beams regularly feature large peak currents but also energy spreads on the percent level. In such a regime, the local energy spread can be reduced by stretching (or decompressing) the electron beam, which linearly reduces the slice energy spread at a moderate cost in peak current. Owing to the ultra-short nature of the electron beam, a comparably compact magnetic chicane is sufficient to stretch the bunch. To increase the Pierce parameter, a specific undulator design was proposed[64]: it minimizes the undulator period and maximizes the undulator parameter K by using a cryogenically cooled in-vacuum design[67,68]. A cryogenic undulator, as described in Ref. [64], is currently being commissioned. With a undulator period of $\lambda_u = 15$ mm and $K = 2-3$, the emitted radiation will be on a 100 nm scale for the 300 MeV electron beam energy, regularly provided by LUX.

6. SIOM

Since 2012, the State Key Laboratory of High Field Laser Physics at SIOM has been building 'the multi-functional ultra-intense ultra-short-pulse laser facility', aiming at developing the compact FEL technology based on the LWFA. A 200 TW Ti:sapphire laser system with 1–5 Hz repetition rate based on chirped pulse amplification was built to drive full coherent FEL[69]. A laser pulse with 800 nm central wavelength was focused to 38 μm (FWHM) onto a gas target by an $f/30$ off-axis parabolic mirror. The gas target is generated from the cascaded or single-stage gas jets because the supersonic flow can generate shock waves or high-density areas, which can be constructed to improve e-beam quality[8,70,71]. In collaboration with SINAP, two sets for FEL experiments have been built, using planar undulators and transverse gradient undulators (TGUs), respectively[72,73], as shown in Figure 5. The TGU scheme reduces the requirement for e-beam energy spread from LWFA[74].

In 2015, 580 MeV high-quality e-beams via energy chirp control were obtained in the experiment, and the maximum six-dimensional brightness is estimated as approximately 6.5×10^{15} A/m^2 per 0.1%, which is very close to the typical brightness of e-beams from state-of-the-art LINAC drivers[70]. However, the energy jitter (>5%) and the pointing jitter (~2 mrad) of the e-beams will affect the commissioning and degrade the FEL gain, especially

https://doi.org/10.1017/hpl.2021.39 Published online by Cambridge University Press

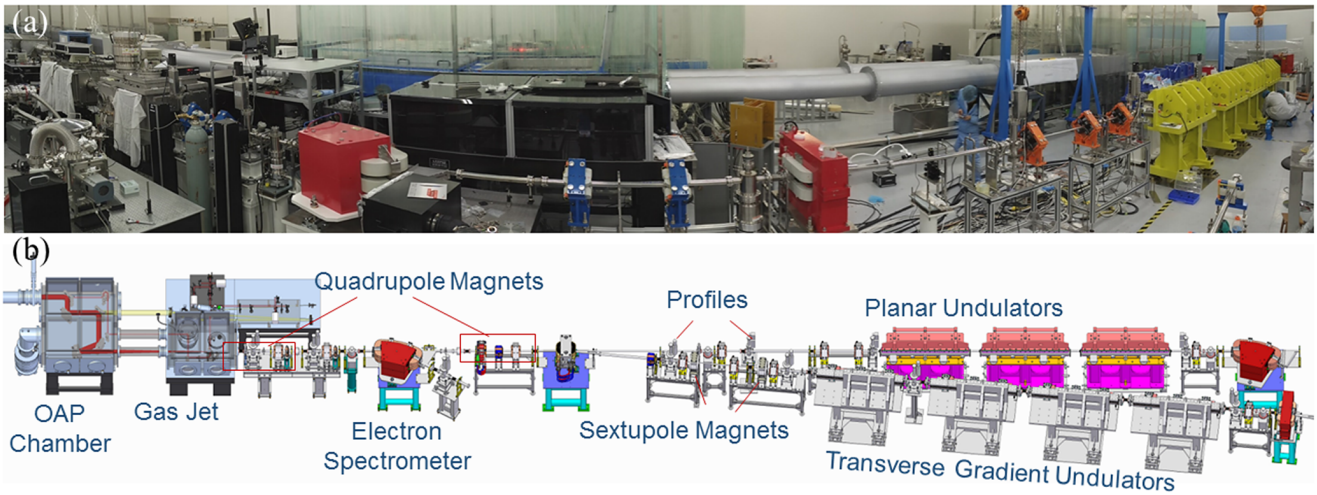

Figure 5. The SIOM-FEL setup with planar undulators and transverse gradient undulators.

in our TGU scheme. Therefore, the subsequent studies focused more on the quality and stability of the e-beams. The 200 TW laser was completely upgraded and almost rebuilt to support e-beam optimization, with the pulse energy fluctuation of less than 0.55% and the beam pointing fluctuation of less than 1.5 μrad in 90 min[75]. Then, a simple, efficient scheme was developed to obtain near-gigaelectronvolt e-beams with energy spreads of few per-mille level in a single-stage LWFA[3]. Longitudinal plasma density was tailored to control relativistic laser-beam evolution, resulting in injection, dechirping, and a quasi-phase stable acceleration. With this scheme, e-beams with peak energies of 780–840 MeV, RMS energy spreads of 0.2%–0.4%, charges of 8.5–23.6 pC, and RMS divergences of 0.1–0.4 mrad were experimentally obtained. Such high-quality e-beams will boost the development of compact intense coherent radiation sources and X-FELs. The further improvement of e-beam quality and stability is very important for the high-gain FEL.

Through simulations, it was established that a portion of the high-quality electron beam could drive amplification of spontaneous emission in a geometry of three undulators, although gain saturation was challenging to be observed. In order to reduce the difficulties in commissioning a first-demonstration compact FEL, a more compact design for beam transport and undulators was used, about 12 m in length, in which only the necessary beam transport and diagnostic devices were retained. This design ensured that the electron beams, as coupled to the three undulators, travelled and maintained a small size over long distances. Recently, the first proof-of-principle demonstration of LWFA-based FEL at around 27 nm was demonstrated[1]. The maximum radiation energy of a single pulse reached 150 nJ, and the maximum obtained gain was approximately 100-fold in the third undulator, as measured by methods of orbit kick and spontaneous radiation calibration. Making the LWFA-based FELs operate in the saturation regime and at shorter wavelengths requires further investigations on the acceleration physics and the undulator beamline designs.

7. Hard plasma-X-FEL (University of Strathclyde *et al.*)

The huge fields in PWFAs do not only enable phase-locked multi-gigaelectronvolt energy gain[5,14], but also generation of ultrahigh-quality electron beams. Plasma photoguns are enabled by the 'Trojan horse' approach[23], wherein a focused laser pulse releases cold electrons via tunnel ionization directly within the plasma wave. These electrons carry negligible transverse momentum and are rapidly compressed and accelerated. Theory and simulation predict normalized beam emittance ε_n of the order of few tens of nanometers rador less in both planes, and kiloamp-level currents I. Such beams display ultrahigh five-dimensional (5D) brightness $B_{5D} = 2I_p/\left(\varepsilon_{n,x}\varepsilon_{n,y}\right)$, orders of magnitude brighter than even in state-of-the-art LINAC-based X-FELs, and thus may enable next-generation X-FELs[76]. The Strathclyde/UCLA-led 'E-210: Trojan Horse PWFA' collaboration had obtained first experimental evidence of the feasibility of plasma photocathodes at SLAC FACET[76]. E-210 has also achieved the first realization of density downramp injection in PWFA[30,76], and opened a door to plasma afterglow metrology, that exploits plasma also for beam diagnostics[77]. A further development of plasma photocathodes allows tailored 'escort' beam loading based energy spread control[78] and dechirping to levels of $(\Delta W/W) \approx 0.01\%$ already at a few gigaelectronvolts, and thus reaching unprecedented six-dimensional (6D) brightness $B_{6D} = B_{5D}/0.1\%\,(\Delta W/W) \approx 10^{21}$ A/(m$^2\cdot$rad$^2\cdot$0.1%bw) in a single accelerator stage. Emittance, 5D and 6D brightness of these bunches would exceed the best state-of-the-art LINAC-based machines by orders of magnitude, would easily overcome the strict requirements of lasing even for very hard X-ray FEL,

https://doi.org/10.1017/hpl.2021.39 Published online by Cambridge University Press

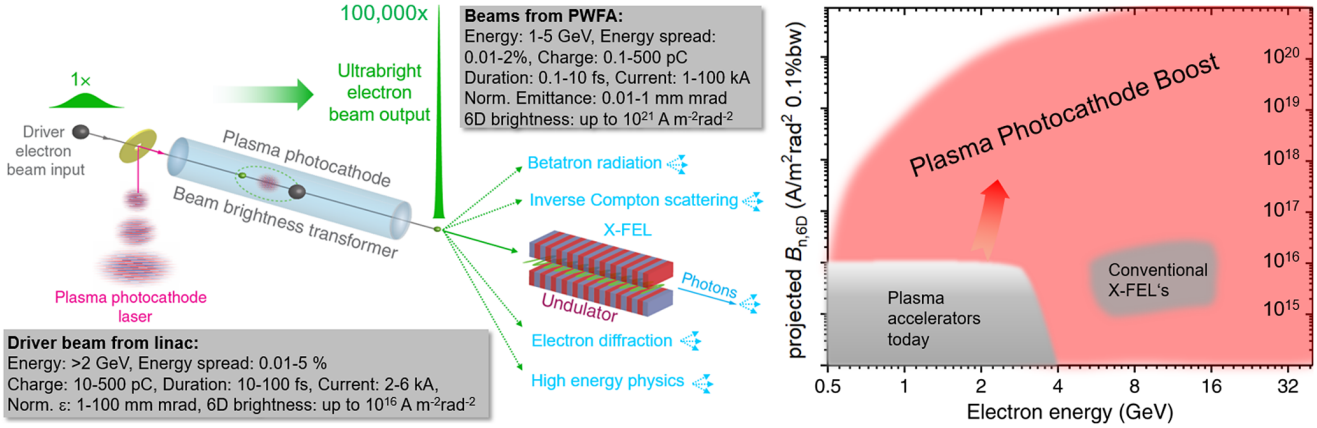

Figure 6. Plasma-based X-FEL and other ultrabright light sources options as summarized in the UK X-FEL science case[81].

and may have a transformative impact on photon science capabilities[79].

Based on the above innovations, the UK STFC 'PWFA-FEL' project[80], a collaboration between Strathclyde, UCLA, ASTeC, and SLAC leads the push for various plasma-X-FEL designs that exploit ultrahigh brightness beams. As a milestone, our plasma-based X-FEL approach is from its conception part of the science case for the UK X-FEL[81], and could be implemented also as a brightness boost afterburner in existing X-FEL facilities such as the LCLS[79].

From the conception of plasma photocathodes 10 years ago and the first vision towards a hard plasma-based X-FEL[23], systematic R&D towards plasma-based X-FEL[82] has included innovations such as multi-color X-FELs and ballistic compression/stretching[83], energy spread control[78], coherent spontaneous emission-based light sources[84], and various other concepts[79,81]. Although a proposal for 'plasma-based hard X-ray FEL with ultrahigh gain and sub-fs capability' at SLAC FACET-II was deemed ahead of its time in 2018, experimental progress on high-brightness beam production from PWFA via the plasma photocathode and plasma torch method at SLAC[30,76] and at DESY via the plasma torch method[85], and from hybrid LWFA→PWFA[86–89], increased confidence in the overall approach[82], and various start-to-end design breakthroughs (A. F. Habib *et al.*, forthcoming) now put dedicated experimental efforts for next-generation electron beam sources for photon science[90] and hard plasma X-FEL on the agenda.

In this context it is helpful that plasma-based X-FELs are now increasingly accepted to be on the map of high-energy and strong-field physics roadmaps[91–93]. The unique ultralow-emittance and ultrahigh-brightness beam potentials of plasma photocathodes are key features for both thrusts due to the importance of emittance and highest beam quality for high-energy physics colliders.

8. LBNL, BELLA Center

The BELLA Center, at the Lawrence Berkeley National Laboratory, houses several laser systems, including a 100 TW-class system called HTU. This 5-Hz, Ti:sapphire-based laser can deliver 800-nm laser pulses on target at 2.5 J energy/pulse and 35 fs pulse duration. An off-axis parabola (focal length of 3 m) enables f/40 focusing to a laser spot of size of 39 μm (intensity FWHM). The gas target for this laser system can be varied, but is most commonly a down-ramp injection target based on a impinging gas flow from a Laval-nozzle with a sharp blade to create the sharp density transition. Figure 7 shows the layout of the system. Following the jet-blade LPA, a series of magnetic 'optics' are applied to transport the electron beam. The LPA and beamline can support electron beams up to 300 MeV.

The core concept behind BELLA Center's approach to plasma-driven FELs is two-fold. (1) To mitigate the intrinsic percent-level energy spread on the LPA beams, a chicane acts as a decompressor[64,65] (making the electron beam longer by longitudinally separating the electrons of various energies). Owing to the unconventional properties of LPA beams (very little R_{56} needed because the beams are ultra-short at the source, but have a relatively large beam size at the chicane), a low-aspect-ratio chicane was developed and commissioned in collaboration with UCLA[94]. (2) To increase the electron beam density over an extended length inside the undulator, the VISA undulator was commissioned for this experiment. The VISA undulator has 16 alternating focusing and defocusing (FODO) quadrupole cells embedded along the 4 m length, providing net focusing in both transverse axes. The inset in Figure 7 shows the optimized beta function (with the square of the beam size proportional to this beta parameter) in the case of (left) perfectly matched delivery into the strong-focusing undulator, (middle) non-ideal mismatched delivery into the strong-focusing undulator, and (right) delivery into a planar undulator without FODO cells. One can

https://doi.org/10.1017/hpl.2021.39 Published online by Cambridge University Press

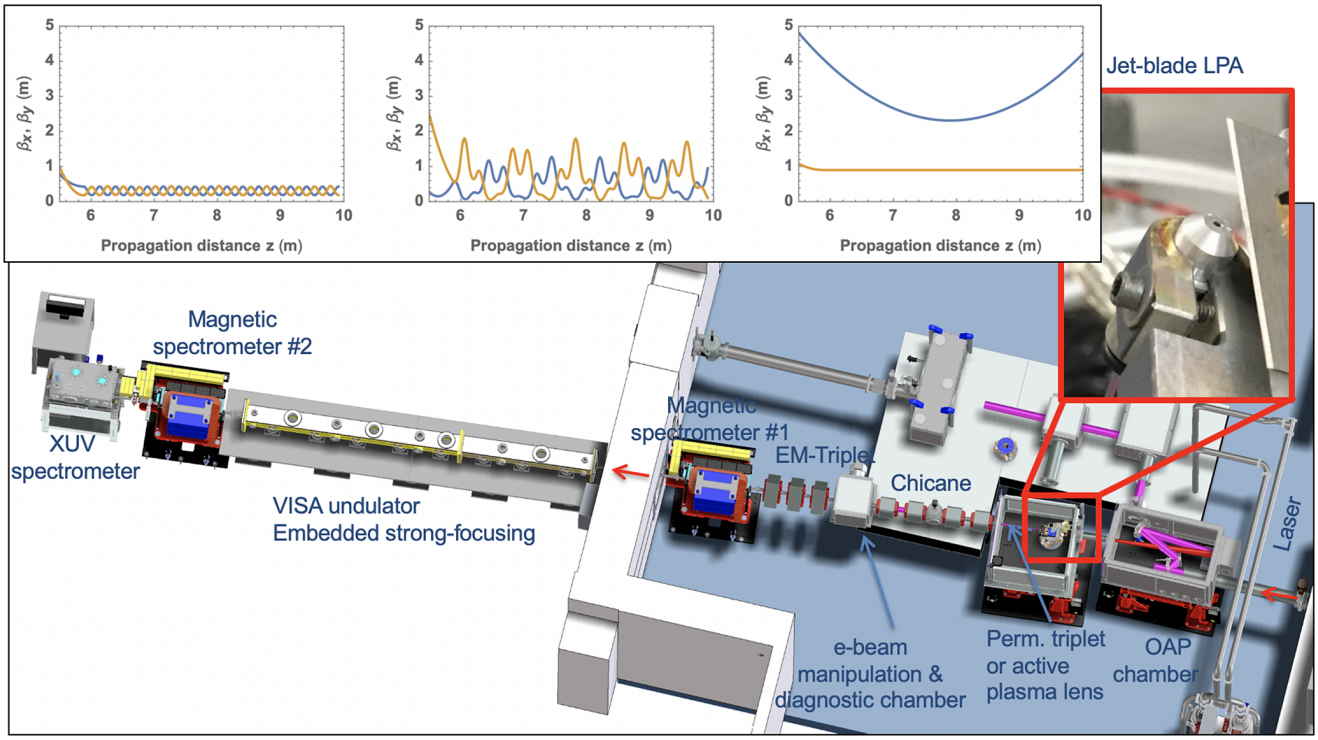

Figure 7. Schematic layout of the BELLA Center's Laser-Plasma Accelerator FEL beamline. The inset shows the electron beam beta function (beam size squared) inside the undulator in (left) the optimally matched strong-focusing undulator, (middle) a mismatched strong-focusing undulator, and (right) an optimized natural-focusing undulator. The strong-focusing undulator allows for higher beam density over the full undulator length.

clearly observe the longitudinally averaged beam density being highest in the first scenario.

In the current phase, electron beam production is tuned to 100 MeV, resulting in 3 eV undulator photon production. Efforts are aimed at integrating better stability and control over the electron beam production and transport, enabled by coupling active stabilization concepts with a new non-perturbative high-power diagnostic of the laser focus position and pointing angle[95].

9. EuPRAXIA at SPARC LAB

The European project EuPRAXIA[87] aims at the construction of an innovative electron accelerator using laser- and electron-beam-driven plasma wakefield acceleration that offers a significant reduction in size and possible savings in cost over current state-of-the-art RF-based accelerators. EuPRAXIA envisions a beam energy of 1–5 GeV and a beam quality (single pulse) equivalent to present RF-based LINACs. Implementation measures have been advanced with a site at the Frascati National Accelerator Laboratory (INFN-LNF) in Italy confirmed, partial funding secured, and it has been recently included in the ESFRI roadmap. EuPRAXIA is supported by a consortium of 40 member institutes and 11 observers, including national accelerator labs and leading institutes and industry. The EuPRAXIA@SPARC_LAB facility[96] at Frascati, aiming to operate a short-wavelength FEL with a beam-driven plasma accelerator module, will be one of the pillars of the EuPRAXIA project. The foreseen layout of the EuPRAXIA@SPARC_LAB infrastructure is schematically shown in Figure 8.

From left to right one can see a 55 m long tunnel hosting a high brightness 150 MeV S-band RF photoinjector equipped with a hybrid compressor scheme based on both velocity bunching and magnetic chicane. The energy boost from 150 MeV up to a maximum 1 GeV will be provided by a chain of high gradient X-band RF cavities. At the LINAC exit, a 5 m long plasma accelerator section will be installed, which includes the plasma module (~0.5 m long capillary with 10^{16} cm^{-3} plasma density) and the required matching and diagnostics sections. In the downstream tunnel, a 40 m long undulator hall is shown, where the undulator chain (with 1.5 cm magnetic period) will be installed. Further downstream after a 31 m long photon diagnostic section the user hall is shown. Additional radiation sources as terahertz and gamma-ray Compton sources are foreseen in the other shown beam lines. The upper room is dedicated to klystrons and modulators to drive the X-band LINAC. The lower light-blue room is where the 300 TW FLAME laser[97] will be installed and eventually upgraded up to 500 TW. The plasma accelerator module can be driven in this layout either by an electron bunch driver (PWFA scheme) or by the FLAME laser itself (LWFA scheme). A staged configuration of both PWFA and LWFA schemes will be also possible in order

https://doi.org/10.1017/hpl.2021.39 Published online by Cambridge University Press

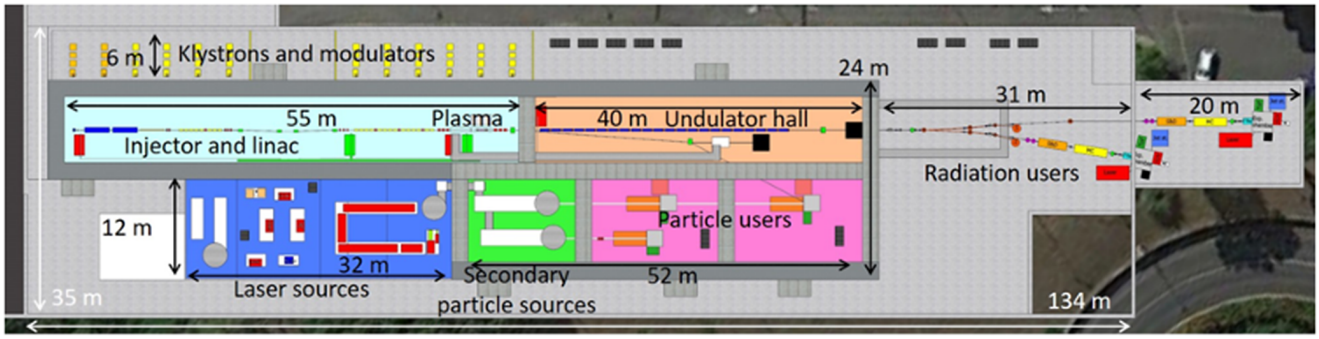

Figure 8. Layout of the EuPRAXIA@SPARC_LAB infrastructure.

to boost the final beam energy in excess of 5 GeV. In addition, FLAME is supposed to drive plasma targets in the green room in order to drive electron and secondary particle sources that will be available to users in the downstream 30 m long user area.

To support the design in both plasma acceleration options (PWFA and LWFA) start-to-end simulations have been performed with promising results, as discussed in the conceptual design report[87]. The reported performances show that this FEL design, driven by a plasma accelerator in SASE configuration, is expected to meet the challenging requests for the new-generation synchrotron radiation sources, producing 10^{12} photons/pulse at 4 nm, in the so-called 'water window' spectral region, by using a 30 pC electron bunch with 3 kA peak current, normalized RMS emittance approximately 1 mm·mrad and energy spread less than 1%. The first foreseen FEL operational mode is based on the SASE mechanism with tapered undulators. More advanced schemes such as seeded and higher harmonic generation configurations will also be investigated. The user end station will be designed and built to allow a wide class of experiments to be performed using the schematic apparatus discussed in Ref. [98]. As a specific example of EuPRAXIA@SPARC_LAB applications it is worth remarking that the FEL radiation in the soft X-ray spectrum opens possibilities for novel imaging methodologies and time-resolved studies in material science, biology, and medicine, along with non-linear optics applications. In this framework the work of SPARC_LAB is of paramount importance, in order to develop new technologies and to study the interaction between beams and plasmas. Recently an energy spread minimization has been achieved[13] at the level of a few per mile . With such a beam we have been able to drive six undulator modules, observing significant light amplification in the FEL process.

10. Conclusion

In this paper we have provided an overview of the main research facilities and university groups actively pursuing research on the path towards developing a plasma-driven FEL. The strong, intercontinental push to pursue this goal is motivated by the possibility of using plasma technology to drastically reduce the physical and economic footprint of current FEL facilities. Concurrently, there are also enticing prospects for improving the performance and adding capabilities to existing FELs by leveraging the unique properties of plasma-accelerated electron beams. These include generating higher-peak-power photon pulses, attosecond X-ray pulses, and operating the FEL at harder X-ray photon energies. The success of these research efforts is predicated on the ability of the community to overcome several key challenges facing plasma-FEL operation. These include continuing improvement of electron beam quality (percent to per-mille energy spread and $\mu m \cdot rad$ to sub-$\mu m \cdot rad$ emittances), increasing the repetition rate from a few hertz to kilohertz and improving the shot-to-shot stability of plasma-accelerated beams.

Impressive progress has already been made and multiple operational facilities are now generating FEL-quality beams with the requisite electron beam parameters for lasing. With the growing confidence gained by the recent first demonstration of plasma-FEL gain, the community looks towards near-term applications of plasma-driven FELs including beginning to serve a user base with dedicated plasma-FEL user facilities. As a result, the outlook for plasma-based FEL operation in the next 5–10 years will involve continuing and strengthening dialogue with the large existing FEL user community to delineate key applications which are best served by plasma-FEL machines. The recent vigorous R&D efforts described in this paper are set to expand global access to FEL photon sources in the next decade, helping to address the demand of the large scientific community currently served by conventional FEL facilities.

References

1. W. Wang, K. Feng, L. Ke, C. Yu, Y. Xu, R. Qi, Y. Chen, Z. Qin, Z. Zhang, Z. J. Zhang, M. Fang, J. Liu, K. N. Jiang, H. Wang, C. Wang, X. Yang, F. Wu, Y. Leng, J. Liu, R. Li, and Z. Xu, Nature **595**, 516 (2021).
2. T. Tajima and J. M. Dawson, Phys. Rev. Lett. **43**, 267 (1979).
3. E. Esarey, C. B. Schroeder, and W. P. Leemans, Rev. Mod. Phys. **81**, 1229 (2009).

https://doi.org/10.1017/hpl.2021.39 Published online by Cambridge University Press

4. P. Chen, J. M. Dawson, R. W. Huff, and T. Katsouleas, Phys. Rev. Lett. **54**, 693 (1985).
5. J. B. Rosenzweig, B. Breizman, T. Katsouleas, and J. J. Su, Phys. Rev. A **44**, R6189 (1991).
6. W. Lu, C. Huang, M. Zhou, W. B. Mori, and T. Katsouleas, Phys. Rev. Lett. **96**, 165002 (2006).
7. A. J. Gonsalves, K. Nakamura, J. Daniels, C. Benedetti, C. Pieronek, T. C. H. de Raadt, S. Steinke, J. H. Bin, S. S. Bulanov, J. van Tilborg, C. G. R. Geddes, C. B. Schroeder, Cs. Toth, E. Esarey, K. Swanson, L. Fan-Chiang, G. Bagdasarov, N. Bobrova, V. Gasilov, G. Korn, P. Sasorov, and W. P. Leemans, Phys. Rev. Lett. **122**, 084801 (2019).
8. L. T. Ke, K. Feng, W. T. Wang, Z. Y. Qin, C. H. Yu, Y. Wu, Y. Chen, R. Qi, Z. J. Zhang, Y. Xu, X. J. Yang, Y. X. Leng, J. S. Liu, R. X. Li, and Z. Z. Xu, Phys. Rev. Lett. **126**, 214801 (2021).
9. A. Buck, M. Nicolai, K. Schmid, C. M. S. Sears, A. Savert, J. M. Mikhailova, F. Krausz, M. C. Kaluza, and L. Veisz, Nat. Phys. **7**, 543 (2011).
10. S. K. Barber, J. van Tilborg, C. B. Schroeder, R. Lehe, H.-E. Tsai, K. K. Swanson, S. Steinke, K. Nakamura, C. G. R. Geddes, C. Benedetti, E. Esarey, and W. P. Leemans, Phys. Rev. Lett. **119**, 104801 (2017).
11. I. Blumenfeld, C. E. Clayton, F.-J. Decker, M. J. Hogan, C. Huang, R. Ischebeck, R. Iverson, C. Joshi, T. Katsouleas, N. Kirby, W. Lu, K. A. Marsh, W. B. Mori, P. Muggli, E. Oz, R. H. Siemann, D. Walz, and M. Zhou, Nature **445**, 741 (2007).
12. C. A. Lindstrøm, J. M. Garland, S. Schroder, L. Boulton, G. Boyle, J. Chappell, R. D'Arcy, P. Gonzalez, A. Knetsch, V. Libov, G. Loisch, A. M. de la Ossa, P. Niknejadi, K. Poder, L. Schaper, B. Schmidt, B. Sheeran, S. Wesch, J. Wood, and J. Osterhoff, Phys. Rev. Lett. **126**, 014801 (2021).
13. R. Pompili, D. Alesini, M. P. Anania, M. Behtouei, M. Bellaveglia, A. Biagioni, F. G. Bisesto, M. Cesarini, E. Chiadroni, A. Cianchi, G. Costa, M. Croia, A. Del Dotto, D. Di Giovenale, M. Diomede, F. Dipace, M. Ferrario, A. Giribono, V. Lollo, L. Magnisi, M. Marongiu, A. Mostacci, L. Piersanti, G. Di Pirro, S. Romeo, A. R. Rossi, J. Scifo, V. Shpakov, C. Vaccarezza, F. Villa, and A. Zigler, Nat. Phys. **17**, 499 (2021).
14. M. Litos, E. Adli, W. An, C. I. Clarke, C. E. Clayton, S. Corde, J. P. Delahaye, R. J. England, A. S. Fisher, J. Frederico, S. Gessner, S. Z. Green, M. J. Hogan, C. Joshi, W. Lu, K. A. Marsh, W. B. Mori, P. Muggli, N. Vafaei-Najafabadi, D. Walz, G. White, Z. Wu, V. Yakimenko, and G. Yocky, Nature **515**, 92 (2014).
15. M. Litos, E. Adli, J. M. Allen, W. An, C. I. Clarke, S. Corde, C. E. Clayton, J. Frederico, S. J. Gessner, S. Z. Green, M. J. Hogan, C. Joshi, W. Lu, K. A. Marsh, W. B. Mori, M. Schmeltz, N. Vafaei-Najafabadi, and V. Yakimenko, Plasma Phys. Control. Fusion **58**, 034017 (2016).
16. V. Shpakov, M. P. Anania, M. Behtouei, M. Bellaveglia, A. Biagioni, M. Cesarini, E. Chiadroni, A. Cianchi, G. Costa, M. Croia, A. Del Dotto, M. Diomede, F. Dipace, M. Ferrario, M. Galletti, A. Giribono, A. Liedl, V. Lollo, L. Magnisi, A. Mostacci, G. Di Pirro, L. Piersanti, R. Pompili, S. Romeo, A. R. Rossi, J. Scifo, C. Vaccarezza, F. Villa, and A. Zigler, Phys. Rev. Accel. Beams **24**, 051301 (2021).
17. R. Bonifacio, C. Pellegrini, and L. Narducci, Opt. Commun. **50**, 373 (1984).
18. M. Xie, in *Particle Accelerator Conference* (IEEE, 1995).
19. V. Yakimenko, L. Alsberg, E. Bong, G. Bouchard, C. Clarke, C. Emma, S. Green, C. Hast, M. J. Hogan, J. Seabury, N. Lipkowitz, B. O'Shea, D. Storey, G. White, and G. Yocky, Phys. Rev. Accel. Beams **22**, 101301 (2019).
20. C. Joshi, E. Adli, W. An, C. E. Clayton, S. Corde, S. Gessner, M. J. Hogan, M. Litos, W. Lu, K. A. Marsh, W. B. Mori, N. Vafaei-Najafabadi, B. O'shea, X. Xu, G. White, and V. Yakimenko, Plasma Phys. Control. Fusion **60**, 034001 (2018).
21. C. L. O'Connell, C. D. Barnes, F.-J. Decker, M. J. Hogan, R. Iverson, P. Krejcik, R. Siemann, D. R. Walz, C. E. Clayton, C. Huang, D. K. Johnson, C. Joshi, W. Lu, K. A. Marsh, W. Mori, M. Zhou, S. Deng, T. Katsouleas, P. Muggli, and E. Oz, Phys. Rev. ST Accel. Beams **9**, 101301 (2006).
22. S. Z. Green, E. Adli, C. I. Clarke, S. Corde, S. A. Edstrom, A. S. Fisher, J. Frederico, J. C. Frisch, S. Gessner, S. Gilevich, P. Hering, M. J. Hogan, R. K. Jobe, M. Litos, J. E. May, D. R. Walz, V. Yakimenko, C. E. Clayton, C. Joshi, K. A. Marsh, N. Vafaei-Najafabadi, and P. Muggli, Plasma Phys. Control. Fusion **56**, 084011 (2014).
23. B. Hidding, G. Pretzler, J. B. Rosenzweig, T. Konigstein, D. Schiller, and D. L. Bruhwiler, Phys. Rev. Lett. **108**, 035001 (2012).
24. X. L. Xu, F. Li, W. An, T. N. Dalichaouch, P. Yu, W. Lu, C. Joshi, and W. B. Mori, Phys. Rev. Accel. Beams **20**, 111303 (2017).
25. C. Emma, X. Xu, A. Fisher, R. Robles, J. P. MacArthur, J. Cryan, M. J. Hogan, P. Musumeci, G. White, and A. Marinelli, APL Photonics **6**, 076107 (2021).
26. J. Duris, S. Li, T. Driver, E. G. Champenois, J. P. MacArthur, A. A. Lutman, Z. Zhang, P. Rosenberger, J. W. Aldrich, R. Coffee, G. Coslovich, F.-J. Decker, J. M. Glownia, G. Hartmann, W , Helml, A. Kamalov, J. Knurr, J. Krzywinski, M.-F. Lin, J. P. Marangos, M. Nantel, A. Natan, J. T. O'Neal, N. Shivaram, P. Walter, A. L. Wang, J. J. Welch, T. J. A. Wolf, J. Z. Xu, M. F. Kling, P. H. Bucksbaum, A. Zholents, Z. Huang, J. P. Cryan, and A. Marinelli, Nat. Photonics **14**, 30 (2019).
27. Z. Zhang, J. Duris, J. P. MacArthur, A. Zholents, Z. Huang, and A. Marinelli, New J. Phys. **22**, 083030 (2020).
28. S. Bulanov, N. Naumova, F. Pegoraro, and J. Sakai, Phys. Rev. E **58**, R5257 (1998).
29. H. Suk, N. Barov, J. B. Rosenzweig, and E. Esarey, Phys. Rev. Lett. **86**, 1011 (2001).
30. D. Ullmann, P. Scherkl, A. Knetsch, T. Heinemann, A. Sutherland, A. F. Habib, O. S. Karger, A. Beaton, G. G. Manahan, A. Deng, G. Andonian, M. D. Litos, B. D. O'Shea, D. L. Bruhwiler, J. R. Cary, M. J. Hogan, V. Yakimenko, J. B. Rosenzweig, and B. Hidding, arXiv:2007.12634 (2020).
31. M.-E. Couprie, A. Loulergue, M. Labat, R. Lehe, and V. Malka, J. Phys. B **47**, 234001 (2014).
32. M. Couprie, M. Labat, C. Evain, C. Szwaj, S. Bielawski, N. Hubert, C. Benabderrahmane, F. Briquez, L. Chapuis, F. Marteau, M. Valléau, O. Marcouillé, P. Marchand, M. Diop, J. L. Marlats, K. Tavakoli, D. Zerbib, L. Cassinari, F. Bouvet, C. Herbeaux, C. Bourassin-Bouchet, D. Dennetière, F. Polack, A. Lestrade, M. Khojoyan, W. Yang, G. Sharma, P. Morin, and A. Loulergue, J. Mod. Opt. **63**, 309 (2016).
33. M. Couprie, M. Labat, C. Evain, F. Marteau, F. Briquez, M. Khojoyan, C. Benabderrahmane, L. Chapuis, N. Hubert, C. Bourassin-Bouchet, M. El Ajjouri, F. Bouvet, Y. Dietrich, M. Valléau, G. Sharma, W. Yang, O. Marcouillé, J. Vétéran, P. Berteaud, T. El Ajjouri, L. Cassinari, C. Thaury, G. Lambert, I. Andriyash, V. Malka, X. Davoine, M. A. Tordeux, C. Miron, D. Zerbib, K. Tavakoli, J. L. Marlats, M. Tilmont, P. Rommeluère, J. P. Duval, M. H. N'Guyen, A. Rouqier, M. Vanderbergue, C. Herbeaux, M. Sebdouai, A. Lestrade, N. Leclercq, D. Dennetière, M. Thomasset, F. Polack, S. Bielawski, C. Szwaj, and A. Loulergue, Plasma Phys. Control. Fusion **58**, 034020 (2016).
34. C. Benabderrahmane, M. Couprie, F. Forest, and O. Cosson, Adjustable magnetic multipole: WO/2016/034490, 3 October 2016 (2016).
35. F. Marteau, A. Ghaith, P. N' Gotta, C. Benabderrahmane, M. Valléau, C. Kitegi, A. Loulergue, J. Vétéran, M. Sebdaoui, T.

https://doi.org/10.1017/hpl.2021.39 Published online by Cambridge University Press

André, G. Le Bec, J. Chavanne, C. Vallerand, D. Oumbarek, O. Cosson, F. Forest, P. Jivkov, J. L. Lancelot, and M. E. Couprie, Appl. Phys. Lett. **111**, 253503 (2017).
36. A. Ghaith, C. Kitegi, T. Andre, M. Valleau, F. Marteau, J. Veteran, F. Blache, C. Benabderrahmane, O. Cosson, F. Forest, P. Jivko, J. L. Lancelot, and M. E. Couprie, Nucl. Instrum. Methods Phys. Res. **909**, 290 (2018).
37. E. Roussel, T. André, I. Andriyash, F. Blache, F. Bouvet, S. Corde, D. Oumbarek Espinos, A. Ghaith, J.-P. Goddet, and C. Kitegi, Plasma Phys. Control. Fusion **62**, 074003 (2020).
38. A. Loulergue, M. Labat, C. Evain, C. Benabderrahmane, V. Malka, and M. E. Couprie, New J. Phys. **17**, 023028 (2015).
39. M. Khojoyan, F. Briquez, M. Labat, A. Loulergue, O. MarcouillE, F. Marteau, G. Sharma, and M. E. Couprie, Nucl. Instrum. Methods Phys. Res. **829**, 260 (2016).
40. A. Ghaith, A. Loulergue, D. Oumbarek, O. Marcouille, M. Valleau, M. Labat, S. Corde, and M.-E. Couprie, Instruments **4**, 1 (2020).
41. M.-E. Couprie, F. Briquez, G. Sharma, C. Benabderrahmane, F. Marteau, O. Marcouillé, P. Berteaud, T. El Ajjouri, J. Vétéran, L. Chapuis, and M. Valléau, Proc. SPIE **9512**, 951204 (2015).
42. C. Benabderrahmane, M. Valleau, A. Ghaith, P. Berteaud, L. Chapuis, F. Marteau, F. Briquez, O. Marcouille, J.-L. Marlats, K. Tavakoli, A. Mary, D. Zerbib, A. Lestrade, M. Louvet, P. Brunelle, K. Medjoubi, C. Herbeaux, N. Bechu, P. Rommeluere, A. Somogyi, O. Chubar, C. Kitegi, and M.-E. Couprie, Phys. Rev. Accel. Beams **20**, 033201 (2017).
43. M. Valléau, F. Briquez, A. Ghaith, F. Marteau, O. Marcouille, C. Kitegi, F. Blache, and M.-E. Couprie, Synchrotron Radiat. News **31**, 42 (2018).
44. M. Labat, M. El Ajjouri, N. Hubert, T. Andre, A. Loulergue, and M.-E. Couprie, J. Synchrotron Radiat. **25**, 59 (2018).
45. C. McGuffey, A. G. R. Thomas, W. Schumaker, T. Matsuoka, V. Chvykov, F. J. Dollar, G. Kalintchenko, V. Yanovsky, A. Maksimchuk, K. Krushelnick, V. Yu. Bychenkov, I. V. Glazyrin, and A. V. Karpeev, Phys. Rev. Lett. **104**, 025004 (2010).
46. A. Pak, K. A. Marsh, S. F. Martins, W. Lu, W. B. Mori, and C. Joshi, Phys. Rev. Lett. **104**, 025003 (2010).
47. T. André, I. A. Andriyash, A. Loulergue, M. Labat, M. Roussel, A. Ghaith, M. Khojoyan, C. Thaury, M. Valleau, F. Briquez, F. Marteau, K. Tavakoli, P. N'Gotta, Y. Dietrich, G. Lambert, V. Malka, C. Benabderrahmane, J. Veteran, L. Chapuis, T. El Ajjouri, M. Sebdaoui, N. Hubert, O. Marcouille, P. Berteaud, N. Leclercq, M. El Ajjouri, P. Rommeluere, F. Bouvet, J. P. Duval, C. Kitegi, F. Blache, B. Mahieu, S. Corde, J. Gautier, K. Ta Phuoc, J. P. Goddet, A. Lestrade, C. Herbeaux, C. Evain, C. Szwaj, S. Bielawski, A. Tafzi, P. Rousseau, S. Smartsev, F. Polack, D. Dennetiere, C. Bourassin-Bouchet, C. De Oliveira, and M. E. Couprie, Nat. Commun. **9**, 1334 (2018).
48. D. O. Espinos, A. Ghaith, A. Loulergue, T. Andre, C. Kitegi, M. Sebdaoui, F. Marteau, F. Blache, M. Valleau, M. Labat, A. Lestrade, E. Roussel, C. Thaury, S. Corde, G. Lambert, O. Kononenko, J.-P. Goddet, A. Tafzi, I. Andriyash, V. Malka, and M.-E. Couprie, Plasma Phys. Control. Fusion **62**, 034001 (2020).
49. A. Ghaith, D. Oumbarek, E. Roussel, S. Corde, M. Labat, T. Andre, A. Loulergue, I. A. Andriyash, O. Chubar, O. Kononenko, S. Smartsev, O. Marcouille, C. Kitegi, F. Marteau, M. Valleau, C. Thaury, J. Gautier, S. Sebban, A. Tafzi, F. Blache, F. Briquez, K. Tavakoli, A. Carcy, F. Bouvet, Y. Dietrich, G. Lambert, N. Hubert, M. El Ajjouri, F. Polack, D. Dennetiere, N. Leclercq, P. Rommeluere, J.-P. Duval, M. Sebdaoui, C. Bourgoin, A. Lestrade, C. Benabderrahmane, J. Veteran, P. Berteaud, C. De Oliveira, J. P. Goddet, C. Herbeaux, C. Szwaj, S. Bielawski, V. Malka, and M.-E. Couprie, Sci. Rep. **9**, 19020 (2019).
50. M. Labat, M. El Ajjouri, N. Hubert, T. Andre, A. Loulergue, and M. E. Couprie, New J. Phys. **25**, 59 (2020).
51. M. Labat, A. Loulergue, T. Andre, I. A. Andriyash, A. Ghaith, M. Khojoyan, F. Marteau, M. Valleau, F. Briquez, C. Benabderrahmane, O. Marcouille, C. Evain, and M. E. Couprie, Phys. Rev. Accel. Beams **21**, 114802 (2018).
52. R. D'Arcy, A. Aschikhin, S. Bohlen, G. Boyle, T. Brummer, J. Chappell, S. Diederichs, B. Foster, M. J. Garland, L. Goldberg, P. Gonzalez, S. Karstensen, A. Knetsch, P. Kuang, V. Libov, K. Ludwig, A. M. de la Ossa, F. Marutzky, M. Meisel, T. J. Mehrling, P. Niknejadi, K. Poder, P. Pourmoussavi, M. Quast, J.-H. Rockemann, L. Schaper, B. Schmidt, S. Schroder, J.-P. Schwinkendorf, B. Sheeran, G. Tauscher, S. Wesch, M. Wing, P. Winkler, M. Zeng, and J. Osterhoff, Philos. Trans. A **377**, 20180392 (2019).
53. W. Ackermann, G. Asova, V. Ayvazyan, A. Azima, N. Baboi, J. Bahr, V. Balandin, B. Beutner, A. Brandt, A. Bolzmann, R. Brinkmann, O. I. Brovko, M. Castellano, P. Castro, L. Catani, E. Chiadroni, S. Choroba, A. Cianchi, J. T. Costello, D. Cubaynes, J. Dardis, W. Decking, H. Delsim-Hashemi, A. Delserieys, G. Di Pirro, M. Dohlus, S. Dusterer, A. Eckhardt, H. T. Edwards, B. Faatz, J. Feldhaus, K. Flottmann, J. Frisch, L. Frohlich, T. Garvey, U. Gensch, Ch. Gerth, M. Gorler, N. Golubeva, H.-J. Grabosch, M. Grecki, O. Grimm, K. Hacker, U. Hahn, J. H. Han, K. Honkavaara, T. Hott, M. Huning, Y. Ivanisenko, E. Jaeschke, W. Jalmuzna, T. Jezynski, R. Kammering, V. Katalev, K. Kavanagh, E. T. Kennedy, S. Khodyachykh, K. Klose, V. Kocharyan, M. Korfer, M. Kollewe, W. Koprek, S. Korepanov, D. Kostin, M. Krassilnikov, G. Kube, M. Kuhlmann, C. L. S. Lewi, L. Lilje, T. Limberg, D. Lipka, F. Lohl, H. Luna, M. Luong, M. Martins, M. Meyer, P. Michelato, V. Miltchev, W. D. Moller, L. Monaco, W. F. O. Muller, O. Napieralski, O. Napoly, P. Nicolosi, D. Nolle, T. Nunez, A. Oppelt, C. Pagani, R. Paparella, N. Pchalek, J. Pedregosa-Gutierrez, B. Petersen, B. Petrosyan, G. Petrosyan, L. Petrosyan, J. Pfluger, E. Plonjes, L. Poletto, K. Pozniak, E. Prat, D. Proch, P. Pucyk, P. Radcliffe, H. Redlin, K. Rehlich, M. Richter, M. Roehrs, J. Roensch, R. Romaniuk, M. Ross, J. Rossbach, V. Rybnikov, M. Sachwitz, E. L. Saldin, W. Sandner, H. Schlarb, B. Schmidt, M. Schmitz, P. Schmuser, J. R. Schneider, E. A. Schneidmiller, S. Schnepp, S. Schreiber, M. Seidel, D. Sertore, A. V. Shabunov, C. Simon, S. Simrock, E. Sombrowski, A. A. Sorokin, P. Spanknebel, R. Spesyvtsev, L. Staykov, B. Steffen, F. Stephan, F. Stulle, H. Thom, K. Tiedtke, M. Tischer, S. Toleikis, R. Treusch, D. Trines, I. Tsakov, E. Vogel, T. Weiland, H. Weise, M. Wellhofer, M. Wendt, I. Will, A. Winter, K. Wittenburg, W. Wurth, P. Yeates, M. V. Yurkov, I. Zagorodnov, and K. Zapfe, Nat. Photonics **1**, 336 (2007).
54. A. R. Maier, N. Delbos, T. Eichner, L. Hubner, S. Jalas, L. Jeppe, S. W. Jolly, M. Kirchen, V. Leroux, P. Messner, M. Schnepp, M. Trunk, P. A. Walker, C. Werle, and P. Winkler, Phys. Rev. X **10**, 031039 (2020).
55. R. D'Arcy, A. Aschikhin, S. Bohlen, G. Boyle, T. Brummer, J. Chappell, S. Diederichs, B. Foster, M. J. Garland, L. Goldberg, P. Gonzalez, S. Karstensen, A. Knetsch, P. Kuang, V. Libov, K. Ludwig, A. M. de la Ossa, F. Marutzky, M. Meisel, T. J. Mehrling, P. Niknejadi, K. Poder, P. Pourmoussavi, M. Quast, J.-H. Rockemann, L. Schaper, B. Schmidt, S. Schroder, J.-P. Schwinkendorf, B. Sheeran, G. Tauscher, S. Wesch, M. Wing, P. Winkler, M. Zeng, and J. Osterhoff, Phys. Rev. Lett. **122**, 034801 (2019).
56. S. Schröder, C. A. Lindstrom, S. Bohlen, G. Boyle, R. D'Arcy, S. Diederichs, M. J. Garland, P. Gonzalez, A. Knetsch, V. Libov, P. Niknejadi, K. Poder, L. Schaper, B. Schmidt, B.

https://doi.org/10.1017/hpl.2021.39 Published online by Cambridge University Press

Sheeran, G. Tauscher, S. Wesch, J. Zemella, M. Zeng, and J. Osterhoff, Nat. Commun. **11**, 5984 (2020).
57. N. Delbos, C. Werle, I. Dornmair, T. Eichner, L. Hubner, S. Jalas, S. W. Jolly, M. Kirchen, V. Leroux, P. Messner, M. Schnepp, M. Trunk, P. A. Walker, P. Winkler, and A. R. Maier, Nucl. Instr. Meth. Phys. Res. A **909**, 318 (2018).
58. V. Leroux, T. Eichner, and A. R. Maier, Opt. Express **26**, 13061 (2018).
59. V. Leroux, T. Eichner, and A. R. Maier, Opt. Express **28**, 8257 (2020).
60. M. Kirchen, S. Jalas, P. Messner, P. Winkler, T. Eichner, L. Hubner, T. Hulsenbusch, L. Jeppe, T. Parikh, M. Schnepp, and A. R. Maier, Phys. Rev. Lett. **126**, 174801 (2021).
61. S. Jalas, M. Kirchen, P. Messner, P. Winkler, L. Hubner, J. Dirkwinkel, M. Schnepp, R. Lehe, and A. R. Maier, Phys. Rev. Lett. **126**, 104801 (2021).
62. R. Lehe, M. Kirchen, I. A. Andriyash, B. B. Godfrey, and J.-L. Vay, Comput. Phys. Commun. **203**, 66 (2016).
63. M. Kirchen, R. Lehe, S. Jalas, O. Shapoval, J.-L. Vay, and A. R. Maier, Phys. Rev. E **102**, 013202 (2020).
64. A. R. Maier, A. Meseck, S. Reiche, C. B. Schroeder, T. Seggebrock, and F. Gruner, Phys. Rev. X **2**, 031019 (2012).
65. C. B. Schroeder, E. Esarey, W. P. Leemans, J. van Tilborg, F. Gruner, A. R. Maier, Y. Ding, and Z. Huang, in *Proceedings of the FEL* 2013 (2013).
66. T. Seggebrock, A. R. Maier, I. Dornmair, and F. Grüner, Phys. Rev. ST Accel. Beams **16**, 070703 (2013).
67. F. Holy, A. R. Maier, B. Zeitler, R. Weingartner, S. Raith, N. Kajumba, M. El Ghazaly, W. Lauth, D. Krambrich, A. Gaupp, M. Scheer, J. Bahrdt, and F. Gruner, Phys. Rev. ST Accel. Beams **17**, 050704 (2014).
68. J. Bahrdt and C. Kuhn, Synchrotron Radiat. News **28**, 9 (2015).
69. Y. Xu, J. Lu, W. Li, F. Wu, Y. Li, C. Wang, Z. Li, X. Lu, Y. Liu, Y. Leng, R. Li, and Z. Xu, Opt. Laser Technol. **79**, 141 (2016).
70. W. T. Wang, W. T. Li, J. S. Liu, Z. J. Zhang, R. Qi, C. H. Yu, J. Q. Liu, M. Fang, Z. Y. Qin, C. Wang, Y. Xu, F. X. Wu, Y. X. Leng, R. X. Li, and Z. Z. Xu, Phys. Rev. Lett. **117**, 124801 (2016).
71. L. Ke, C. Yu, K. Feng, Z. Qin, K. Jiang, H. Wang, S. Luan, X. Yang, Y. Xu, Y. Leng, W. Wang, J. Liu, and R. Li, Appl. Sci. **11**, 2560 (2021).
72. T. Liu, T. Zhang, D. Wang, and Z. Huang, Phys. Rev. Accel. Beams **20**, 020701 (2017).
73. T. Liu, C. Feng, D. Xiang, J. Liu, and D. Wang, J. Synchrotron Radiat. **26**, 311 (2019).
74. Z. Huang, Y. Ding, and C. B. Schroeder, Phys. Rev. Lett. **109**, 204801 (2012).
75. F. Wu, Z. Zhang, X. Yang, J. Hu, P. Ji, J. Gui, C. Wang, J. Chen, Y. Peng, X. Liu, Y. Liu, X. Lu, Y. Xu, Y. Leng, R. Li, and Z. Xu, Opt. Laser Technol. **131**, 106453 (2020).
76. A. Deng, O. S. Karger, T. Heinemann, A. Knetsch, P. Scherkl, G. G. Manahan, A. Beaton, D. Ullmann, G. Wittig, A. F. Habib, Y. Xi, M. D. Litos, B. D. O'Shea, S. Gessner, C. I. Clarke, S. Z. Green, C. A. Lindstrom, E. Adli, R. Zgadzaj, M. C. Downer, G. Andonian, A. Murokh, D. L. Bruhwiler, J. R. Cary, M. J. Hogan, V. Yakimenko, J. B. Rosenzweig, and B. Hidding, Nat. Phys. **15**, 1156 (2019).
77. P. Scherkl, A. Knetsch, T. Heinemann, A. Sutherland, A. F. Habib, O. Karger, D. Ullmann, A. Beaton, G. Kirwan, G. Manahan, Y. Xi, A. Deng, M. D. Litos, B. D. O'Shea, S. Z. Green, C. I. Clarke, G. Andonian, R. Assmann, D. A. Jaroszynski, D. L. Bruhwiler, J. Smith, J. R. Cary, M. J. Hogan, V. Yakimenko, J. B. Rosenzweig, and B. Hidding, arXiv:1908.09263 (2019).
78. G. Manahan, A. F. Habib, P. Scherkl, P. Delinikolas, A. Beaton, A. Knetsch, O. Karger, G. Wittig, T. Heinemann, Z. M. Sheng, J. R. Cary, D. L. Bruhwiler, J. B. Rosenzweig, and B. Hidding, Nat. Commun. **8**, 15705 (2017).
79. A. F. Habib, P. Scherkl, G. G. Manahan, T. Heinemann, D. Ullmann, A. Sutherland, A. Knetsch, M. Litos, M. Hogan, J. Rosenzweig, and B. Hidding, Proc. SPIE **11110**, 111100A (2019).
80. https://pwfa-fel.phys.strath.ac.uk/.
81. J. Marangos, A. Burnett, M. Borghesi, A. Comley, M. Dean, S. Diaz-Moreno, D. Dye, J. Greenwood, A. Higginbotham, A. Kirrander, J. Marangos, M. McMahon, R. Minns, M. Newton, A. Orville, T. Penfold, A. Regoutz, I. Robinson, D. Rugg, S. Schroeder, J. van Thor, S. Vinko, S. Wall, J. Wark, J. Weinstein, A. Zair, X. Zhang, J. Clarke, J. Collier, L. Cowie, D. Dunning, J. Green, N. Thompson, P. W. M. Altarelli, F. A. Lima, M. Attallah, S. Bartlett, J. Baxter, U. Bergmann, T. Blackburn, R. Boll, S. Bonetti, C. Bressler, B. Brocklesby, C. Brown, P. Bucksbaum, R. Catlow, R. Chantrell, A. Cohen, S. Coles, J. Cryan, G. Dakovski, S. Dhesi, J. Dyke, D. Eakins, G. Evans, M. Foerst, L. Frasinski, G. Gregori, M. Guehr, F. Habib, D. Hall, S. Hasnain, T. Heinzl, B. Hidding, S. Hooker, N. Huse, O. Johansson, D. Keen, P. Kolorenc, A. Mancuso, S. Mangles, M. Marklund, S. Matthews, S. McWilliams, M. McCoustra, P. McKenna, C. Milne, H. Mueller-Werkmeister, S. Mukamel, J. Naismith, K. Nelson, A. Ourmazd, R. Owen, F. Perakis, P. Radaelli, D. Riley, A. Robinson, J. Rodenberg, N. Rohringer, K. Rossnagel, M. Ruberti, C. Russo, C. Sanders, M. Scheck, P. Scherkl, C. Schofield, R. Scott, E. Snell, E. Springate, D. Stuart, G. Thornton, J. von Zanthier, M. Walsh, M. Warren, P. Weber, and J. Yano, UK XFEL Science Case (Science and Technology Facilities Council, 2020).
82. B. Hidding, G. G. Manahan, O. Karger, A. Knetsch, G. Wittig, D. A. Jaroszynski, Z.-M. Sheng, Y. Xi, A. Deng, J. B. Rosenzweig, G. Andonian, A. Murokh, G. Pretzler, D. L. Bruhwiler, and J. Smith, J. Phys. B **47**, 234010 (2014).
83. B. Hidding, O. Karger, G. Wittig, C. Aniculaesei, D. Jaroszynski, B. W. J. McNeil, L. T. Campbell, M. R. Islam, B. Ersfeld, Z.-M. Sheng, Y. Xi, A. Deng, J. B. Rosenzweig, G. Andonian, A. Murokh, M. J. Hogan, D. L. Bruhwiler, and E. Cormier, arXiv:1403.1109 (2014).
84. B. Alotaibi, R. Al tuijri, F. Habib, A. Hala, B. Hidding, S. M. Khalil, B. McNeil, and P. Traczykowski, New J. Phys. **22**, 013037 (2020).
85. A. Knetsch, B. Sheeran, L. Boulton, P. Niknejadi, K. Põder, L. Schaper, M. Zeng, S. Bohlen, G. Boyle, T. Brümmer, J. Chappell, R. D'Arcy, S. Diederichs, B. Foster, M. J. Garland, P. G. Caminal, B. Hidding, V. Libov, C. A. Lindstrøm, A. M. de la Ossa, M. Meisel, T. Parikh, B. Schmidt, S. Schröder, G. Tauscher, S. Wesch, P. Winkler, J. Wood, and J. Osterhoff, arXiv:2007.12639 (2020).
86. B. Hidding, T. Konigstein, J. Osterholz, S. Karsch, O. Willi, and G. Pretzler, Phys. Rev. Lett. **104**, 195002 (2010).
87. R. Assmann, M. K. Weikum, T. Akhter, D. Alesini, A. S. Alexandrova, M. P. Anania, N. E. Andreev, I. Andriyash, M. Artioli, A. Aschikhin, T. Audet, A. Bacci, I. F. Barna, S. Bartocci, A. Bayramian, A. Beaton, A. Beck, M. Bellaveglia, A. Beluze, A. Bernhard, A. Biagioni, S. Bielawski, F. G. Bisesto, A. Bonatto, L. Boulton, F. Brandi, R. Brinkmann, F. Briquez, F. Brottier, E. Bru, M. Buscher, B. Buonomo, M. H. Bussmann, G. Bussolino, P. Campana, S. Cantarella, K. Cassou, A. Chance, M. Chen, E. Chiadroni, A. Cianchi, F. Cioeta, J. A. Clarke, J. M. Cole, G. Costa, M.-E. Couprie, J. Cowley, M. Croia, B. Cros, P. A. Crump, R. D'Arcy, G. Dattoli, A. Del Dotto, N. Delerue, M. Del Franco, P. Delinikolas, S. De Nicola, J. M. Dias, D. Di Giovenale, M. Diomede, E. Di Pasquale, G. Di Pirro, G. Di Raddo, U. Dorda, A. C. Erlandson, K. Ertel, A. Esposito, F. Falcoz, A. Falone, R. Fedele, A. F. Pousa, M. Ferrario, F. Filippi, J. Fils, G. Fiore, R. Fiorito,

https://doi.org/10.1017/hpl.2021.39 Published online by Cambridge University Press

R. A. Fonseca, G. Franzini, M. Galimberti, A. Gallo, T. C. Galvin, A. Ghaith, A. Ghigo, D. Giove, A. Giribono, L. A. Gizzi, F. J. Gruner, A. F. Habib, C. Haefner, T. Heinemann, A. Helm, B. Hidding, B. J. Holzer, S. M. Hooker, T. Hosokai, M. Hubner, M. Ibison, S. Incremona, A. Irman, F. Iungo, F. J. Jafarinia, O. Jakobsson, D. A. Jaroszynski, S. Jaster-Merz, C. Joshi, M. Kaluza, M. Kando, O. S. Karger, S. Karsch, E. Khazanov, D. Khikhlukha, M. Kirchen, G. Kirwan, C. Kitegi, A. Knetsch, D. Kocon, P. Koester, O. S. Kononenko, G. Korn, I. Kostyukov, K. O. Kruchinin, L. Labate, C. Le Blanc, C. Lechner, P. Lee, W. Leemans, A. Lehrach, X. Li, Y. Li, V. Libov, A. Lifschitz, C. A. Lindstrom, V. Litvinenko, W. Lu, O. Lundh, A. R. Maier, V. Malka, G. G. Manahan, S. P. D. Mangles, A. Marcelli, B. Marchetti, O. Marcouille, A. Marocchino, F. Marteau, A. M. de la Ossa, J. L. Martins, P. D. Mason, F. Massimo, F. Mathieu, G. Maynard, Z. Mazzotta, S. Mironov, A. Y. Molodozhentsev, S. Morante, A. Mosnier, A. Mostacci, A.-S. Muller, C. D. Murphy, Z. Najmudin, P. A. P. Nghiem, F. Nguyen, P. Niknejadi, A. Nutter, J. Osterhoff, D. O. Espinos, J.-L. Paillard, D. N. Papadopoulos, B. Patrizi, R. Pattathil, L. Pellegrino, A. Petralia, V. Petrillo, L. Piersanti, M. A. Pocsai, K. Poder, R. Pompili, L. Pribyl, D. Pugacheva, B. A. Reagan, J. Resta-Lopez, R. Ricci, S. Romeo, M. R. Conti, A. R. Rossi, R. Rossmanith, U. Rotundo, E. Roussel, L. Sabbatini, P. Santangelo, G. Sarri, L. Schaper, P. Scherkl, U. Schramm, C. B. Schroeder, J. Scifo, L. Serafini, G. Sharma, Z. M. Sheng, V. Shpakov, C. W. Siders, L. O. Silva, T. Silva, C. Simon, C. Simon-Boisson, U. Sinha, E. Sistrunk, A. Specka, T. M. Spinka, A. Stecchi, A. Stella, F. Stellato, M. J. V. Streeter, A. Sutherland, E. N. Svystun, D. Symes, C. Szwaj, G. E. Tauscher, D. Terzani, G. Toci, P. Tomassini, R. Torres, D. Ullmann, C. Vaccarezza, M. Valleau, M. Vannini, A. Vannozzi, S. Vescovi, J. M. Vieira, F. Villa, C.-G. Wahlstrom, R. Walczak, P. A. Walker, K. Wang, A. Welsch, C. P. Welsch, S. M. Weng, S. M. Wiggins, J. Wolfenden, G. Xia, M. Yabashi, H. Zhang, Y. Zhao, J. Zhu, and A. Zigler, Eur. Phys. J. Spec. Top. **229**, 3675 (2020).

88. M. F. Gilljohann, H. Ding, A. Dopp, J. Gotzfried, S. Schindler, G. Schilling, S. Corde, A. Debus, T. Heinemann, B. Hidding, S. M. Hooker, A. Irman, O. Kononenko, T. Kurz, A. M. de la Ossa, U. Schramm, and S. Karsch, Phys. Rev. X **9**, 011046 (2019).
89. T. Kurz, T. Heinemann, M. F. Gilljohann, Y. Y. Chang, J. P. C. Cabadağ, A. Debus, O. Kononenko, R. Pausch, S. Schobel, R. W. Assmann, M. Bussmann, H. Ding, J. Gotzfried, A. Kohler, G. Raj, S. Schindler, K. Steiniger, O. Zarini, A. Dopp, B. Hidding, S. Karsch, U. Schramm, A. M. de la Ossa, and A. Irman, Nat. Commun. **12**, 2895 (2021).
90. https://nexource.phys.strath.ac.uk/.
91. B. Hidding, S. Hooker, S. Jamison, B. Muratori, C. Murphy, Z. Najmudin, R. Pattathil, G. Sarri, M. Streeter, C. Welsch, M. Wing, and G. Xia, arXiv:1904.09205 (2019).
92. B. Hidding, B. Foster, M. J. Hogan, P. Muggli, and J. B. Rosenzweig, Philos. Trans. A **377**, 20190215 (2019).
93. The European Strategy Group, "Deliberation Document on the 2020 update of the European Strategy for Particle Physics," Report No. CERN-ESU-014 (2020).
94. N. Majernik, S. K. Barber, J. van Tilborg, J. B. Rosenzweig, and W. P. Leemans, Phys. Rev. Accel. Beams **22**, 032401 (2019).
95. F. Isono, J. van Tilborg, S. K. Barber, J. Natal, C. Berger, H.-E. Tsai, T. Ostermayr, A. Gonsalves, C. Geddes, and E. Esarey, High Power Laser Sci. Eng. **9**, e25 (2021).
96. M. Ferrario, D. Alesini, M. P. Anania, M. Artioli, A. Bacci, S. Bartocci, R. Bedogni, M. Bellaveglia, A. Biagioni, F. Bisesto, F. Brandi, E. Brentegani, F. Broggi, B. Buonomo, P. L. Campana, G. Campogiani, C. Cannaos, S. Cantarella, F. Cardelli, M. Carpanese, M. Castellano, G. Castorina, N. C. Lasheras, E. Chiadroni, A. Cianchi, R. Cimino, F. Ciocci, D. Cirrincione, G. A. P. Cirrone, R. Clementi, M. Coreno, R. Corsini, M. Croia, A. Curcio, G. Costa, C. Curatolo, G. Cuttone, S. Dabagov, G. Dattoli, G. D'Auria, I. Debrot, M. Diomede, A. Drago, D. Di Giovenale, S. Di Mitri, G. Di Pirro, A. Esposito, M. Faiferri, L. Ficcadenti, F. Filippi, O. Frasciello, A. Gallo, A. Ghigo, L. Giannessi, A. Giribono, L. Gizzi, A. Grudiev, S. Guiducci, P. Koester, S. Incremona, F. Iungo, L. Labate, A. Latina, S. Licciardi, V. Lollo, S. Lupi, R. Manca, A. Marcelli, M. Marini, A. Marocchino, M. Marongiu, V. Martinelli, C. Masciovecchio, C. Mastino, A. Michelotti, C. Milardi, V. Minicozzi, F. Mira, S. Morante, A. Mostacci, F. Nguyen, S. Pagnutti, L. Pellegrino, A. Petralia, V. Petrillo, L. Piersanti, S. Pioli, D. Polese, R. Pompili, F. Pusceddu, A. Ricci, R. Ricci, R. Rochow, S. Romeo, J. B. Rosenzweig, M. R. Conti, A. R. Rossi, U. Rotundo, L. Sabbatini, E. Sabia, O. S. Plannell, D. Schulte, J. Scifo, V. Scuderi, L. Serafini, B. Spataro, A. Stecchi, A. Stella, V. Shpakov, F. Stellato, E. Turco, C. Vaccarezza, A. Vacchi, A. Vannozzi, A. Variola, S. Vescovi, F. Villa, W. Wuensch, A. Zigler, and M. Zobov, Nucl. Instrum. Methods Phys. Res. A **909**, 134 (2018).
97. F. Bisesto, M. P. Anania, M. Bellaveglia, E. Chiadroni, A. Cianchi, G. Costa, A. Curcio, D. Di Giovenale, G. Di Pirro, M. Ferrario, F. Filippi, A. Gallo, A. Marocchino, R. Pompili, A. Zigler, and C. Vaccarezza, Nucl. Instrum. Methods Phys. Res. A **909**, 452 (2018).
98. Istituto Nazionale di Fisica Nucleare, "EuPRAXIA@ SPARC_LAB Conceptual Design Report", LNF-18/03 (2018).

https://doi.org/10.1017/hpl.2021.39 Published online by Cambridge University Press